HYDROTHERMAL SYNTHESIS OF HETEROSTRUCTURED Ag_3PO_4/TiO_2 PHOTOCATALYST WITH ENHANCED PHOTOCATALYTIC ACTIVITY AND STABILITY UNDER VISIBLE LIGHT

Z. SONG[*], Y. Q. HE

College of Chemistry, Changchun Normal University, Changchun 130032, Jilin, People's Republic of China

Photocatalyst Ag_3PO_4/TiO_2 composites were synthesized by hydrothermal method, by adding 0 ml, 0.1 ml, 0.2 ml, 0.3 ml ammonia to adjust the morphology of Ag_3PO_4 and change the mass ratio of Ag_3PO_4 to TiO_2 (10%, 20%, 30%. % means mass ratio of Ag_3PO_4 to TiO_2). Ag_3PO_4 was recrystallized in the shape-controlled process which provides chance for TiO_2 injected to the internal Ag_3PO_4. The obtained composites were characterized by XRD, FT-IR, SEM, EDS. This study found that the catalytic efficiencyis of 10% Ag_3PO_4/TiO_2 (added 0.2 ml ammonia) (10%-A/T-0.2) is the best. The photocatalysts were investigated in methyl orange (MO) under visible irradiation ($\lambda \geq 420$nm). Compared to pure TiO_2 and Ag_3PO_4 crystals, the heterostructured Ag_3PO_4/TiO_2 composites show much higher photocatalytic activity and stability. Moreover, after three cycles of photocalytic experiment found that photodegradation rate of MO still reach 72.59% in 60 minutes, indicating that the as-prepared heterostructured Ag_3PO_4/TiO_2 photocatalysts are stable. The enhanced and stability photocatalytic of Ag_3PO_4/TiO_2 could mainly account of its highly heterojunction and high efficient separation of photogenerated electron-hole pairs.

1. Introduction

Coincident with the development of the dye synthesis and printing industry, the semiconductor photocatalysts have attracted considerable attention due to its great potential for resolving the current energy and environmental problems [1-6]. Most of dyes are based on complex organic structure. Because of their complex structures, the dyes are very difficult to degrade completely, which will cause huge environmental pollution. Since the TiO_2 was first reported in 1972 [7-8], TiO_2 photocatalysis technology as a new environmental protection technology had been widely research. But the forbidden band width of TiO_2 (Eg = 3.2 eV) of the absorption of light accounts for only 4%-5% of the sunlight [9-10], the visible light utilization rate is very low. In 2010, Ye and co-workers [11-12] first reported Ag_3PO_4 as photocatalyst. Many research results also show that Ag_3PO_4 has superior photocatalytic properties, because forbidden band width of the Ag_3PO_4 is only 2.36 eV and the quantum efficiency of solar energy up to 90% [12]. However, Ag_3PO_4 has low photocatalytic stability under visible light irradiation and cost a great deal fortune in synthesized process, which limited its use in solving the environmental problems. Fortunately, a few attempts have been made to solve such these problems by combining of Ag_3PO_4 with different materials. For insistence, AgX (X=Cl, Br, I)/Ag_3PO_4 [13], carbon quantum-Ag_3PO_4, graphene/Ag_3PO_4 [14], carbon quantum dots/Ag_3PO_4 [15] have been considered to be promising photocatalysts. Yao and co-workers [16] using the carrier of PM25 through adsorption precipitation synthesis Ag_3PO_4/TiO_2 nanocatalyst for the first time. Through chemical bath deposition, Yang [17] using TiO_2 nanotube arrays as the carrier, obtained Ag_3PO_4/TiO_2

_____
[*] Corresponding author: songzheszh@126.com

nanocomposites. Rawal [18], mix Ag_3PO_4 nanoparticles in precursor of TiO_2, obtained Ag_3PO_4/TiO_2 composite materials.

To our knowledge, there are few research reports about different morphology of Ag_3PO_4/TiO_2 nanocomposites catalytic activity. Structures determine properties, so this experiment by adding ammonia as a structure-directing agent to adjust the morphology of Ag_3PO_4 (including spherical, polyhedral spherical, gyro, and strip). Importantly, ammonia plays a vital role in the hedrothermal process. NH_3 was escape from ammonia at high temperature and capture the Ag^+ formed $Ag(NH_3)_2^+$ then recrystallized new morphology of Ag_3PO_4 with PO_4^{3-} under the condition of hydrothermal method. In this recrystallized process, provide chance for TiO_2 injected to the internal Ag_3PO_4. So, the coupled high heterostructured Ag_3PO_4/TiO_2 nanocomposites were obtained.

2. Experimental

2.1. Materials

Anhydrous ethanol, Titanium dioxide, silver nitrate were purchased from Beijing Chemical Company, China. Sodium phosphate dodecahydrate, 25wt% ammonia solution was purchased from Tianjin Yongda Reagents Co. Ltd., China. Milli-Q water (resistivity >18.0 MΩ·cm) was used throughout the experiments. All the medicines were of AR grade and used without further purification.

2.2. Hydrothermal sythesis of heterostructured Ag_3PO_4/TiO_2 nanocomposites

Sythesis of 10% Ag_3PO_4/TiO_2 (0.2 ml ammonia) (10%-A/T-0.2): 0.306g of $AgNO_3$ was dissolved in 5 ml deionized water forms A solution on the electromagnetic stirrer. 0.228g of $Na_3PO_4·12H_2O$ dissolved in 5 ml deionized water and on the electromagnetic stirrer forms B solution. 0.1 ml ammonia dissolved in 4.8 ml deionized water forms C (the total volume of C solution is 5.0 ml). C solution is transferred into A formed D solution. 2.540 g of TiO_2 was dispersed in D solution. Then under dark condition, B solution was added dropwise in the above solution within 30 minutes stirring. Finally, the obtained mixtures was transferred into a Teflon-lined stainless steel autoclave (filling degree of 60%) and maintained at 423 K for 24 h. Cooling to room temperature, separation, precipitation and using water, absolute ethanol respectively wash three times with the centrifuge (5000 r/min), and dried in oven at 343K for 12 hours, 10%-A/T-0.2 composite was obtained. For comparison, the 10% Ag_3PO_4/TiO_2 (0 ml, 0.1 ml, 0.3 ml ammonia) were obtained under the same conditions, and the mass ratio of 20% Ag_3PO_4/TiO_2, 30% Ag_3PO_4/TiO_2 (the volume of ammonia was added 0 ml, 0.1 ml, 0.2 ml, 0.3 ml) were obtained. Such 12 different compounds were obtained.

The as-prepared samples were termed with "X-A/T-x", X means the mass ratio of Ag_3PO_4 to TiO_2, x represents the volume of ammonia from 0.0 ml to 0.3 ml, in addition, Ag_3PO_4 was labeled "A" and TiO_2 was labeled "T". The twelve samples were labeled as 10%-A/T-0.0, 10%-A/T-0.1, 10%-A/T-0.2, 10%-A/T-0.3, 20%-A/T-0.0, 20%-A/T-0.1, 20%-A/T-0.2, 20%-A/T-0.3, 30%-A/T-0.0, 30%-A/T-0.1, 30%-A/T-0.2, and 30%-A/T-0.3.

The pure Ag_3PO_4 was obtained under the same conditions without the addition of TiO_2.

2.3. Photocatalytic degradation of methyl orange performance study

Photocatalytic reaction system is composed under visible light from a 300W Xe lamp light source equipped with one ultraviolet cut off (λ≥420nm), magnetic stirrer, The temperature of reaction solution was maintained at 298K by thermostatic bath. Typically, 0.05 g of photocatalyst powder was dispersed in 100 ml of 10 mg/L of methyl orange (MO) aqueous solution. Under the condition of dark stirring for 40 min, it made the system to reach adsorption equilibrium between the photocatalyst and dye aqueous solution. During the photocatalytic degradation progress, 2 ml samples were taken out at each given time intervals and separated through centrifugation (5000 rpm, 10 min) to remove the catalysts. Supernatants were evaluated by a UV-1600 ultraviolet-visible spectrophotometer, and the upper clear solution was measured at a wavelength of 466 nm. After each cycle, the photocatalyst was washed with water and absolute ethanol three times,

respectively and dried at 343K for 12 h.

2.4. Catalyst characterization

The X-ray powder diffraction (XRD) patterns of the samples were recorded on a D8-Advance X-ray diffractometer with Cu Kα (λ=0.15406nm) radiation with scanning angles of 10°-80°.The applied current and accelerating voltage were 40 mA and 30 kV , respectively. Scanning electron microscopy (SEM) images were tested by a SU8000 scanning electron microscope operated at 15 kV. Energy dispersive spectrometer (EDS) was analyzed on a SU8000 scanning electron microscope. FT-IR spectra were tested on an Excalibur HE 3100 infrared spectrometer.

3. Results and discussion

3.1. Characterization

In order to determine the crystal phase composition of the photocatalysts, the XRD analysis was carried out. Fig.1 shows the XRD patterns of the Ag_3PO_4/TiO_2 composites. For comparison, the XRD patterns of pure TiO_2 and pure Ag_3PO_4 were also carried out. From these patterns, over Ag_3PO_4, the obvious diffraction peaks at 20.92º, 29.74º, 33.36º, 36.66º, 42.55º, 47.88º, 52.76º, 55.12º, 57.41º, 61.74º, 65.77º, 69.85º, 71.82º, 73.78º can be indexed to crystallite planes of (110), (200), (210), (211), (220), (310), (222), (320), (321), (400), (411), (421), (332). As for the TiO_2, the strong diffraction peaks at 25.3º, 37.05º, 37.91º, 38.67º, 48.16º, 54.05º, 55.20º, 62.30º, 62.87º, 70.48º, 75.28º, 76.25º can be indexed into crastallite planes of (101), (103), (004), (112), (200), (105), (211), (213), (204), (220), (215), (301). Over Ag_3PO_4/TiO_2 composites, characteristic peak of Ag_3PO_4 and TiO_2 are observed.
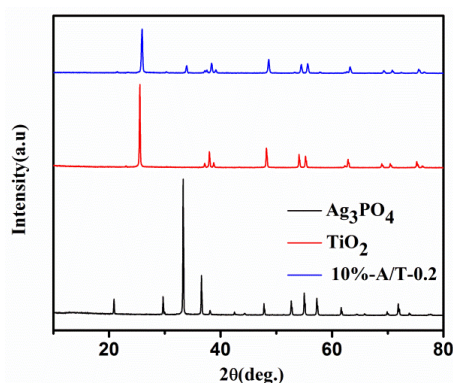
Fig. 1 XRD patterns of pure Ag_3PO_4 and TiO_2, 10%-A/T-0.2 composites
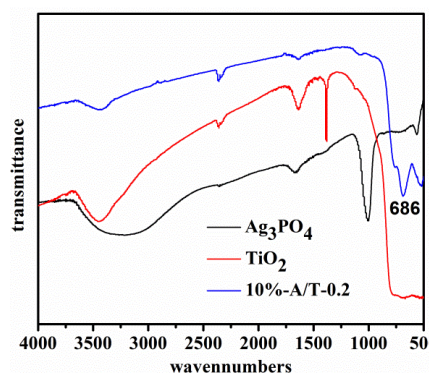
Fig.2 FTIR spectra of the TiO_2, Ag_3PO_4, 10%-A/T-0.2 in the regions of 4000-500 cm^{-1}
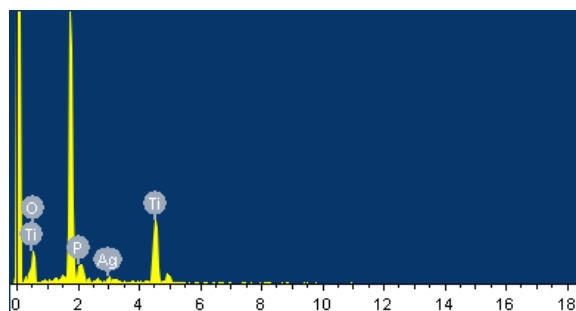
Fig.3 The EDS pattern of 10% -A/T-0.2

According to the XRD diffraction peaks, indicating that compounds crystal formed well. Further investigation was carried out by FT-IR and EDS methods. The pure TiO_2, Ag_3PO_4, and 10%A/T-0.2 were analyzed by means of FT-IR and EDS methods. Fig.2 shows the obtained FT-IR spectra. In TiO_2 sample, a strong and broad absorption at 3443 cm^{-1} was observed, which could be assigned to the stretching vibration and bending vibration of ·OH on the surface of TiO_2. Another peak at 1636 cm^{-1} was attributed to the bending vibration of the adsorbed H_2O on the surface of TiO_2. The broad absorption at around 500-700 cm^{-1} is the characteristic peaks of TiO_2. Over the pure Ag_3PO_4, two strong absorption peaks at 1010 cm^{-1} and 550 cm^{-1} were observed, which were corresponding to the P-O stretching vibration of phosphate (PO_4^{3-}) [19]. Over the composites of 10%-A/T-0.2, a new peak at 686 cm^{-1} was observed, indicating that there was a heterojunction between Ag_3PO_4 and TiO_2 was formed. Moreover, The EDS pattern of 10%-A/T-0.2 was shown in Fig.3. The elements of O, P, Ti, and Ag were further proved the samples should be assigned to the composites of 10%-A/T-0.2, which were corresponding to the XRD patterns.

3.2. Morphology Analysis

Fig.4 shows SEM images of the pure Ag_3PO_4. The Ag_3PO_4 from the beginning of the morphology of spherical turned into polyhedral spherical, gyro with the volume of 0 ml, 0.1 ml, 0.2 ml, until 0.3 ml ammonia, was completely changed into a strip to a large extent. As the picture shown (see Fig.4), surface of Ag_3PO_4 had a lot of particals, and it suggested that an obvious secondary nucleation and growth were existed. According to the experimental results found that added 0.2 ml ammonia catalytic activity was the best. By comparing electron microscopy (SEM) images of Fig.5 (a) and Fig.5 (b), the heterojunction of 10%-A/T-0.2 formed most closely between Ag_3PO_4 and TiO_2, which further to prove ammonia play a decisive role in the process. On the basis of the above results, a likely formation mechanism of the reaction was proposed (see Scheme 1).
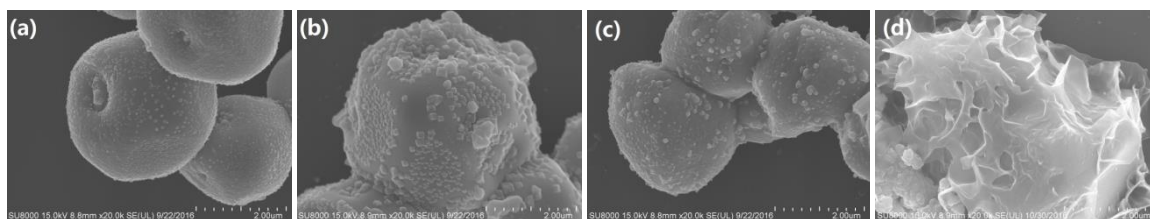
Fig.4 SEM image of samples: (a) Ag_3PO_4 (0 ml ammonia); (b) Ag_3PO_4 (0.1 ml ammonia);

(c) Ag_3PO_4 (0.2 ml ammonia); (d) Ag_3PO_4 (0.3 ml ammonia)
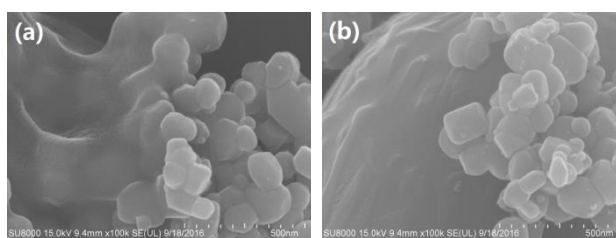
Fig.5 (a) SEM images of 10% -A/T-0.2 (b) SEM images of 10% -A/T-0.0

3.3. Photocatalytic activity test

The photocatalytic activity of Ag_3PO_4/TiO_2 was tested through degrading MO under visible light ($\lambda \geq 420nm$) at room temperature. The absolution of MO at approximately 466 nm was used to monitor the process of degradation. As the Fig. 6 (a), (b), (c), (d) showed the samples were respectively introduced 0 ml, 0.1ml, 0.2 ml, 0.3ml ammonia into the mass ratio of Ag_3PO_4/TiO_2 from 10% to 30%. The data showed 10%-A/T had much higher photocatalytic activity than 20%-A/T and 30%-A/T. Moreover, Fig.7 (a) illustrated that the 10%-A/T-0.2 had the best photocatalytic performance. Fig.7 (b) can see the pure Ag_3PO_4 and TiO_2 photocatalytic activity, and TiO_2 had no visible light activity because of its weak absolution under near visible light region, but the Ag_3PO_4 displayed good photocatalytic activity for degrading MO. However, Fig. 8 (b) shows that the stability of Ag_3PO_4 in the reaction process was not good in the second recycling experiment. On the contrary, 10%-A/T-0.2 had the best photocatalytic performance for degrading MO, nearly 100% MO was degraded in 60 minutes and had good stability (see Fig.8 (a)).
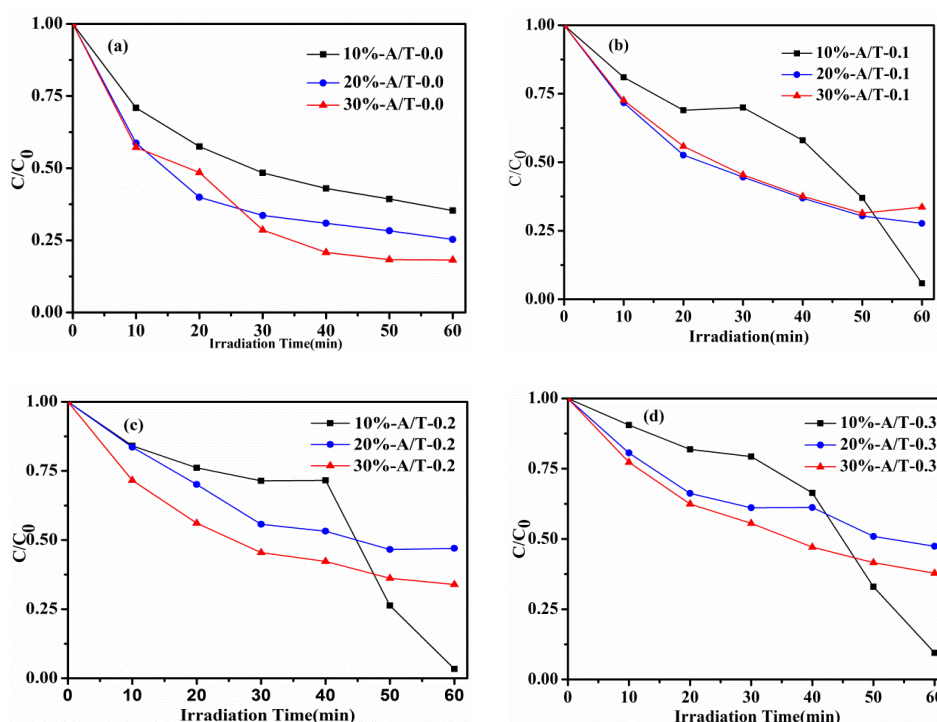
Fig.6 (a) 10%-A/T-0.0, 20%-A/T-0.0, 30%-A/T-0.0; (b) 10%-A/T-0.1, 20%-A/T-0.0, 30%-A/T-0.0;
(c) 10%-A/T-0.2, 20%-A/T-0.2, 30%-A/T-0.3; (d) 10%-A/T-0.3, 20%-A/T-0.3, 30%-A/T-0.3
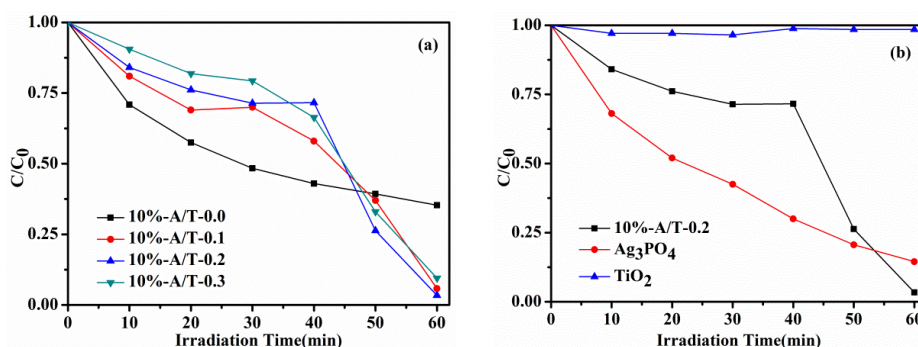
Fig. 7 (a) 10%-A/T-0.0, 10%-A/T-0.1, 10%-A/T-0.2, 10%-A/T-0.3;
(b) Pure TiO_2 and pure Ag_3PO_4 and 10%-A/T-0.2
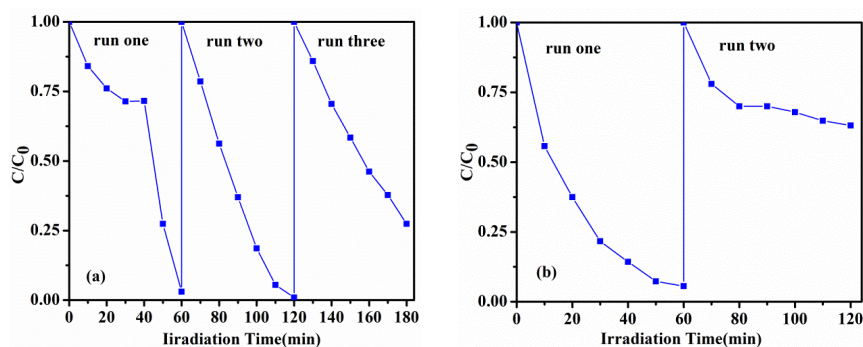
Fig. 8 (a) The cycling degradation for MO of 10%-A/T-0.2
(b) The cycling degradation for MO of pure Ag_3PO_4

The stability of 10%-A/T-0.2 in the reaction process was invested through three times recycling experiments. Fig.8 (a) (b) show that the photocatalytic performance of 10%-A/T-0.2 still kept high photocatalytic activity. After three cycles of photocalytic experiment found that degradation rate ($E=1-C/C_0$, E the degradation rate of MO, C_0 the initial concentration of MO) up to 72.59% in 60 minutes, still higher than pure Ag_3PO_4 and TiO_2, and it indicates that 10%-A/T-0.2 displays better visible-light photocatalytic stability than pure Ag_3PO_4 and TiO_2. This confirms that the heterostructures can improved the degradation rate of dyes and stability.

3.4. Reaction mechanism

On the basis of above results and aforementioned discussion, a possible formation mechanism of obtained high stability heterocatalyst 10%-A/T-0.2 was proposed. The SEM images (see Fig.4) demonstrated that the morphology of Ag_3PO_4 was changed when added ammonia vary from 0 ml, 0.1 ml, 0.2 ml, 0.3 ml. To our knowledge, previously reported that NH_3 gases can escape from urea ($CO(NH_2)_2$) at high temperature. The morphology of Ag_3PO_4 was adjusted from microrod to tetrapod [20]. Hence, in this paper, we conjecture that the NH_3 was escape from ammonia at high temperature and capture the Ag^+ formed $Ag(NH_3)_2^+$ then recrystallized new morphology of Ag_3PO_4 with PO_4^{3-} under the condition of hydrothermal method. In the recrystallization process, TiO_2 can insert to the Ag_3PO_4. As a result, the stability heterocatalyst was obtained (the process of reaction mechanism can see Scheme 1). Compared SEM images of Fig. 5(a) and Fig. 5(b), as it clears that there was no heterojuction without adding ammonia sample. Further demonstrated the heterojunction between Ag_3PO_4 and TiO_2 the NH_3 play a decisive role.

$$TiO_2 + NH_3 \cdot H_2O + Ag_3PO_4 \text{ (Spherical)} \longrightarrow TiO_2 + Ag(NH_3)_2^+ + PO_4^{3-} \qquad (1)$$

$$TiO_2 + PO_4^{3-} + Ag(NH_3)_2^+ \longrightarrow \text{ heterostructured } Ag_3PO_4/TiO_2 \qquad (2)$$
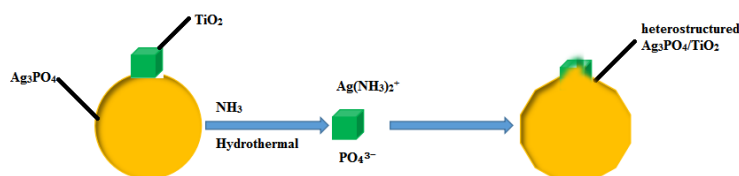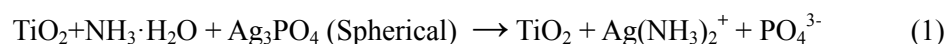
Scheme 1. Schematic representation of the growth mechanism of 10%-A/T-0.2 heterostructures

As literature recorded, the conduction band (CB) and valence band (VB) potentials of Ag_3PO_4 (CB=0.45eV, VB=2.88eV) [11] are more active than TiO_2 (CB= -0.11 eV, VB=2.89 eV) [21]. In this case, Ag_3PO_4 was irradiated by visible light the electron leaped into the CB and left behind a hole in the VB. In the heterostructured Ag_3PO_4/TiO_2 photocatalyst, due to the VB level of Ag_3PO_4 was lower than TiO_2, the photogenerated holes on the surface of Ag_3PO_4 can migrate to the VB of TiO_2. At the same time, the electrons of TiO_2 could also migrate to the surface of Ag_3PO_4. The photogenerated can generate $\cdot O^{2-}$ and other active radicals, and produced $\cdot OH$ and other active radicals over the surface of the composites catalyst reacted with water, which was mainly responsible in oxidizing the organic compounds. The photocatalytic can inhibit the recombination of electron-hole due to special heterostructured. As a result, our heterocatalyst 10%-A/T-0.2 exhibited highly activity and stability than pure TiO_2 and pure Ag_3PO_4. The possible mechanism of enhanced photocatalytic stability and activity could be show in scheme 2.
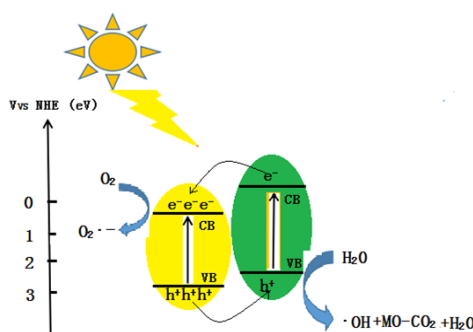
Scheme 2. The possible mechanism for enhanced visible-light photocatalytic stability and activity

4. Conclusions

In summary, by adjusting the ammonia concentration during the hydrothermal method, the morphology of Ag_3PO_4 can be turned via a recrystallization process. Furthermore, the TiO_2 can co-precipitation in the recrystallization process and obtained the p-n junction heterocatalyst. The 10%-A/T-0.2 shows higher efficient photocatalytic activity and stability compared with pure Ag_3PO_4, TiO_2. Especially, because of the coupling of Ag_3PO_4 and TiO_2 restrained the opportunity of recombination of photogenerated electrons (e-) and holes (h+), 10%-A/T-0.2 presents excellent stability with a degradation of 72.59% after three cycles, which demonstrated an effective heterocatalyst was obtained. As a result, the high stability heterocatalyst 10%-A/T-0.2 will have

promise application in environmental protection. More importantly, the above experiments find that mass ratio only 10% the photocatalytic performance is the best, significantly reducing the cost of pure Ag_3PO_4 photocatalyst.

Acknowledgments

References

[1] H. Tong, S. X. Ouyang, Y.P. Bi, N. Umezawa, I. Oshikiri, J.H. Ye Adv. Mater. **24,** 229 (2012).

[2] C. L. Yu, W. Q. Zhou, Q. Z. Fan, L. F. Wei, J. C. Chen, J. C. Yu China J. Catal. **34,** 1250 (2013).

[3] J.D. Li, W. Fang, C.L. Yu, W.Q. Zhou, L.H. Zhu, Y. Xie Appl. Surf. Sci., **358,** 46 (2015).

[4] J.J. Tian, H.P. Gao, H.M. Deng, L. Sun, H. Kong, P.X. Yang, J.H. Chu J. Alloys Compd. **581,** 318 (2013).

[5] H. Liu, L. Deng, C.C. Sun, J.P. Li, Z.F. Zhu Appl. Surf. Sci. **326**, 82 (2015).

[6] B. ZENG, W. ZENG. DIG J NANOMATER BIOSD. **11**, 1105 (2016).

[7] A. Fujishima, X. Zhang, D.A. Tryk Surf. Sci. Rep. **63,** 515 (2008).

[8] A. Fujishima, K. Honda Nature. **238,** 37 (1972).

[9] S. Protti, A. Albini, N. Serpone Phys. Chem. Chem. Phys. **16,** 19790 (2014).

[10] S.G. Kumar, L.G. Devi J. Phys. Chem. A **115,** 13211 (2011).

[11] Z. Yi, J. Ye, N. Kikugawa Nat. Mater. **9,** 559 (2010).

[12] Y. Bi, S. Ouyang, N. Umezawa J. Am. Chem. Soc. **133**, 6490 (2011).

[13] Y. Bi, S. Ouyang, J. Cao Phys. Chem. Chem. Phys. **13,** 10071 (2011).

[14] Q. Liang, Y. Shi, W. Ma, Z. Li, X. Yang Phys. Chem. Chem. Phys. **14,** 15657 (2012).

[15] H. Zhang, H. Huang, H. Ming, H. Li, L. Zhang, Y. Liu, et al. J. Mater. Chem. **22,** 10501 (2012).

[16] W. Yao, B. Zhang, C. Huang J. Mater. Chem. **22,** 4050 (2012).

[17] J. Xie, Y. Yang, H. He, D. Cheng, M. Mao, Q. Jiang, L. Song, J. Xiong Appl. Surf. Sci. **355,** 921 (2015).

[18] S.B. Rawal, S.D. Sung, W.I. Lee Catal. Commun. **17,** 131(2012).

[19] K. Vivekanandan, S. Selvasekarapandian, P. Kolandaivel Mater. Chem. Phys. **39,** 284 (1995).

[20] J. Wang, F. Teng, M.D. Chen, J.J. Xu, Y.Q. Song, X.L. Zhou, Crysta Eng Comm **15,** 39 (2013).

[21] C. Yu, L. Wei, J. Chen, Y. Xie, W. Zhou, Q. Fan Ind. Eng. Chem. Res. **53,** 5759 (2014).